Hindawi Publishing Corporation
Mathematical Problems in Engineering
Volume 2016, Article ID 4170371, 8 pages
http://dx.doi.org/10.1155/2016/4170371

Research Article

Dimensional Analysis of Average Diameter of Bubbles for Bottom Blown Oxygen Copper Furnace

Dongxing Wang, Yan Liu, Zimu Zhang, Pin Shao, and Ting'an Zhang

School of Metallurgy of Northeastern University, Key Laboratory of Ecological Utilization of Multi-Metal Intergrown Ores of Education Ministry, Shenyang 110819, China

Correspondence should be addressed to Yan Liu; shanqibao2000@163.com

Received 8 March 2016; Accepted 21 July 2016

Academic Editor: Giuseppe Vairo

Average diameter of bubbles is important in copper furnace. Based on the principle of similarity, a slice water model of a furnace with bottom-blown oxygen in matte-smelting process was established. A high-speed camera was used to record images continuously and clearer pictures were selected for treatment. Finally, image processing software was used for obtaining the average diameter of the bubbles. The effects of different injection conditions and equipment factors such as the diameter of nozzle, the nozzle installing angle, and gas velocity on the average diameter of bubbles were studied with cold water model experiment, exploring the dispersion and disintegration rules of bubbles. According to experimental data and Buckingham's theorem, by using dimensional analysis method, an empirical formula on average diameter of bubbles was established ($d_B = 0.41666 d^{0.29374} \theta^{-0.46572} \nu^{-0.16725}$). It can be seen from the formula that nozzle installing angle and diameter of nozzle make the most impact on the average diameter of bubbles in bottom blown oxygen copper furnace.

1. Introduction

About 80% of copper is produced by pyrometallurgical process. The other 20% is obtained by hydrometallurgy. Pyrometallurgical process includes matte smelting, converting, fire refining, and electrorefining of blister copper [1]. The objective of the smelting process is to melt concentrate and oxidize S and Fe in the concentrate and produce matte (a Cu-enriched molten sulfide phase) containing 50~75% copper. The molten matte is processed in a converter resulting in crude copper of 98.5~99.5% copper content [2]. Converting is mostly carried out in the cylindrical Peirce-Smith converter. Oxygen-enriched air is often used as the oxidant.

Bath smelting is one of the most important matte smelting techniques with oxygen-enriched air blown into the matte, including top blown such as Ausmelt and Isa smelt, side blown such as Noranda and Teniente process, and bottom blown such as SKS process.

Injection technology is widely used in hot metal pretreatment, strengthening the reaction in furnace, secondary refining of liquid steel, and other fields. In converter steelmaking, for example, mixing time of top blowing is 90 to 120 seconds, of bottom blowing is only 10 to 20 seconds, and top and bottom combined blowing is 20~50 seconds. From this, we can see a significant advantage of bottom blowing.

The bottom blown technique has been widely used in the steel industry, such as oxygen bottom blown converter; oxygen is blown into the molten pool through the bottom of the converter and makes molten iron smelting into steel. The technique of blowing argon from the bottom of ladle takes advantage of the stirring effect of bottom blown argon, making the composition and temperature of liquid steel uniform and the inclusions and bubbles in steel rise quickly, thus increasing the purity of liquid steel [3, 4]. In the field of nonferrous metallurgy industry, the application of bottom blown technique is very limited, which is mainly used for lead smelting and copper smelting [5–8].

In recent years, oxygen bottom blown copper smelting technology (SKS) has been used more and more widely in China. SKS includes two generations of technology; the first is "bottom blown smelting-PS furnace converting" and the second is "bottom blown smelting-bottom blown continuous converting."

SKS process has many advantages such as high oxygen enrichment, low temperature, and autothermal operation. It has a very strong adaptability of raw materials; the preparation of raw material is very simple. It can directly deal with the wet material, block material, and garbage material. Its thermal efficiency is very high, without additional fuel. This new technology has great potential for expanding production capability and energy saving [8–10]. Since the first bottom blown oxygen copper furnace was put into production in 2008, there will be more than 8 bottom blown furnaces running in China in 2015.

Bottom blown oxygen copper smelting process is a new technology whose significant feature is the application of high speed bottom jet. From the viewpoint of metallurgical reaction engineering, the bath smelting method can be divided into two kinds, namely, the bubble bath smelting and jetting bath smelting. When the oxygen-enriched air is injected from tuyere into the bath at a low velocity, the air is actually sprayed into the molten pool at a pulse type, belonging to the bubble generation system, namely, the bubble bath smelting. When the oxygen-enriched air is blown from tuyere into the bath at a high velocity, approaching or exceeding sonic velocity, the air is blown into the molten pool at stability state of continuous injection, belonging to the jet system, namely, the jetting bath smelting.

For jetting blown, the air separates into many small bubbles. The smaller bubble diameter means the larger gas-liquid boundary area at the same quantity of gas. With small bubbles, molten pool has no fierce nuisance spitting, so small bubbles are helpful to extend the service life of the refractory material.

In bath smelting process with gas injection, the size, rising velocity, and dispersion of the bubbles, and the gas holdup have enormous influence on the interface reaction or multiphase reaction, directly affecting the reaction rate and oxygen utilization. Besides, the residence time of smaller bubbles is longer.

A large number of studies have been carried out on the investigation of the flow regimes in submerged gas injection. Davidson and coworkers [11, 12] formulated a theoretical model of continuous bubble formation at submerged orifices in water model. They resulted in the relationship between bubble volume, V, and gas flow rate, G: $V = 1.138G^{1.2}\,g^{-0.6}$. A camera was used to take the photographs of the bubble formation. The mean volume of bubbles measured from the photographs. Hoefele and Brimacombe [13] investigated the behavior of gas injected into liquids by high-speed cinematography and pressure measurement in the tuyere. They found that matte converters are in the bubbling regime. Tests on an operating nickel converter confirmed that with low pressure blowing practice air discharges into the bath in the form of large bubbles whose corresponding diameters are 400 mm at room temperature. The bubble frequency is between 10 and 12 s^{-1}. Bustos et al. [14] thought the blockage of tuyeres and the life of the refractory lining in a side-blown air copper converter are related to the injection of air. Bubble volume and equivalent radius must be considered. In the Peirce-Smith copper converter, bubbles growing at adjacent tuyeres coalesce to form a horizontal unstable gas envelope. If the tuyere submergence is shallower than 300 mm, bubbles may break through the bath surface and form a vertical channel. Then the oxygen utilization is poor.

Valencia et al. [15] had numerically studied the fluid dynamics in a model of Teniente type copper converter with combined lateral and bottom injection. The volume fraction of water distribution, velocity vectors, agitation of bath surface, and gas penetration in three different models was studied. With the help of bottom injection, the model produced more jet interaction, bath inner agitation, and mixing. Zhao and Irons [16] used K-H and R-T instability theory to explain the breakup of a bubble forming at a submerged nozzle. They present the first theory to predict the transition from bubbling to jetting for submerged gas injection.

Lou et al. [17] studied the formation and motion rules of bubbles in Isasmelt furnace by water model and numerical simulation method. Their conclusion is that, with the increase of gas flow rate Q, the bubble frequency decreases and the bubble diameter increases. When the gas flow rate Q is equal to 24 m^3/h, the equivalent diameter d of the bubble is about 25 mm, and residence time of bubble ranges from 0.14 to 0.16 s.

Bottom blown oxygen copper smelting process is still in a development stage with many shortcomings and deficiencies [8–10]. It is high speed jetting blowing and different from side-blown Peirce-Smith copper converter and other traditional bubble bath smelting. The mechanisms of high speed bottom jet still need to be studied which is very important for the improvement of the process. The air injected into the molten pool will break up into many small bubbles; there is very little research about the process, such as the dispersion and size of bubbles, the factors which influence bubbles size and their relationship.

In this paper, a water model of the bottom blown furnace was produced to study the mean bubble diameter in the SKS process. Some effects of variables on the bubbles dispersions and gas holdup were researched in our former paper [18]. This paper mainly analyzes the relationship between the parameters and derived the empirical equation of mean bubble diameter. From empirical equation, the effects of the diameter of nozzle, the nozzle installing angle, and gas velocity on the average diameter of bubbles were studied.

2. Experimental

2.1. Principles. For geometric similarity, a water model with a scale down of 1 : 5 was built. The main geometrical sizes of the model were proportional to those of the prototype.

Dynamic similarity relies on the fact that the modified Froud number Fr′ between the model and prototype should be equal. Using (1), the quantity of gas injected into the model can be calculated:

$$Q_m = \left(\frac{\rho_{gp}}{\rho_{gm}} \cdot \frac{\rho_{lm}}{\rho_{lp}} \cdot \frac{d_m^4}{d_p^4} \cdot \frac{H_m}{H_p} \right)^{1/2} \cdot Q_p, \tag{1}$$

Table 1: Attributes of model and materials.

System	Radius of the pool/mm	Width of the pool/mm	Height of liquid level/mm	Density of liquid/(kg·m^{-3})	Density of gas/(kg·m^{-3})
Water model	342	300	342	1000	1.25
Prototype	1710	15000	1710	4600	1.37

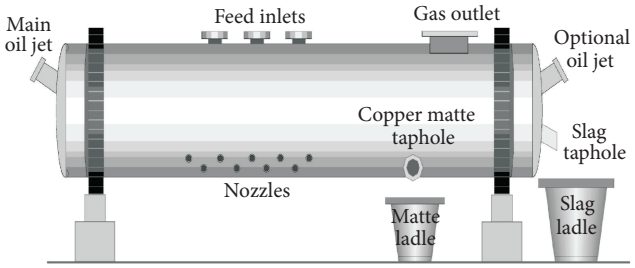

Figure 1: Bottom blown oxygen copper smelting furnace.

Figure 2: Sketch of experimental setup.

where ρ stands for the density; d is the diameter of nozzle; H is the depth of the pool; Q stands for the quantity of injected gas; the subscripts p, m, l, and g stand for the prototype, model liquid, and gas, respectively.

2.2. Apparatus. The water model used in our experiment references a company's bottom blown oxygen copper smelting furnace as shown in Figure 1. The external diameter of the furnace is 4.4 m which lined with 380 mm thickness refractory bricks and the length is 16.5 m. Nine nozzles are installed on the bottom of the furnace in two rows. For the convenience of observation, a cross-sectional model which contains only one nozzle was built up. The specifications are shown in Table 1. The material of the model is organic glass. Inside diameter of the model is 684 mm and as a cross-sectional model the length is 300 mm, so that the experiment phenomena can be easily observed from the cross section.

Water model is shown in Figure 2. There are different positions on the bottom of the model for nozzles to be installed.

2.3. Experimental Procedure and Methods. The model was half full with water and air was injected into the water from the nozzles on the bottom of the model. Combined with high-speed camera, image processing technology is an important method to study the characteristics of bubbles [19]. A high-speed camera was used to record the experimental phenomena continuously; single frame images with bubbles could be obtained for the water model experiment. Clearer pictures were selected, then identifiable bubbles were marked, and the edges were reinforced treatment. Finally, image processing software was used for obtaining the mean diameter of the bubbles.

2.4. Dimensional Analysis. Dimensional analysis is an important method to research the relationships of variables that describe the physical phenomena. The foundation of dimensional analysis is that the empirical and rational equations must be dimensionally homogeneous, which means both sides of an equation must have the same units [20]. In engineering, empirical formula between the parameters can be derived from experiment data by the method of dimensional analysis which also enabled weighing the magnitude of each operating parameter [21]. For example, by the means of dimensional analysis, Yan et al. [22] obtained a penetration depth criterion equation of 1/2 anode structure electrolytic cell.

3. Dimensional Analysis of Average Diameter of Bubbles

Through water model experiments, the average diameter of bubbles was obtained. By the method of dimensional analysis, the influence of different experimental conditions on the average diameter of bubbles can be studied and the fitting equation was obtained.

Considering the main factors that affect bubbles in the experiments, according to Buckingham's theorem (π-principle), the independent variables were found out.

The average diameter of bubbles d_B was mainly affected by the following factors:

(1) The diameter of the nozzle d.

(2) The height of liquid level H.

(3) The angle between the nozzle and horizontal plane θ.

(4) The diameter of the model D.

(5) The gas pressure P.

(6) The viscosity of water μ_l.

(7) The viscosity of gas μ_g.

(8) The gas-liquid interfacial tension $\sigma_{g\text{-}l}$.

(9) The density of water ρ_l.

Table 2: Dimension of variable.

	d_B	d	H	θ	D	P	μ_l	μ_g	$\sigma_{g\text{-}l}$	ρ_l	ρ_g	g	v
M	0	0	0	0	0	1	1	1	1	1	1	0	0
L	1	1	1	0	1	−1	−1	−1	0	−3	−3	1	1
T	0	0	0	0	0	−2	−1	−1	−2	0	0	−2	−1

(10) The density of gas ρ_g.

(11) The acceleration of gravity g.

(12) The gas velocity v.

By the above analysis, using dimensional analysis we can draw general functional form as follows:

$$d_B = f\left(d, H, \theta, D, P, \mu_l, \mu_g, \sigma_{g\text{-}l}, \rho_l, \rho_g, g, v\right). \tag{2}$$

Or

$$f\left(d_B, d, H, \theta, D, P, \mu_l, \mu_g, \sigma_{g\text{-}l}, \rho_l, \rho_g, g, v\right) = 0. \tag{3}$$

The variable dimension is listed in Table 2.

By the analysis of π-principle, the total number of variables is 13 and the number of independent variables is $k = 3$, so that $n - k = 10$ dimensionless quantity can be set up [22–24]. ρ_l, H, and μ_l were selected as independent variables:

$$\begin{aligned} \dim \rho_l &= M^{\alpha_1} L^{\beta_1} T^{\gamma_1} = M^1 L^{-3} T^0, \\ \dim H &= M^{\alpha_2} L^{\beta_2} T^{\gamma_2} = M^0 L^1 T^0, \\ \dim \mu_l &= M^{\alpha_3} L^{\beta_3} T^{\gamma_3} = M^1 L^{-1} T^{-1}, \end{aligned} \tag{4}$$

$$\begin{vmatrix} \alpha_1 & \beta_1 & \gamma_1 \\ \alpha_2 & \beta_2 & \gamma_2 \\ \alpha_3 & \beta_3 & \gamma_3 \end{vmatrix} = \begin{vmatrix} 1 & -3 & 0 \\ 0 & 1 & 0 \\ 1 & -1 & -1 \end{vmatrix} = -1 \neq 0. \tag{5}$$

Because (5) is not equal to 0, ρ_l, H, and μ_l are independent of each other and it is reasonable that they were selected as independent variables. For the variables d_B, d, and D, as they only contain length dimension, therefore in the construction of dimensionless Π, they can be directly expressed with the dimensionless independent variable H. Each Π is expressed as follows:

$$\begin{aligned} \Pi_0 &= \frac{d_B}{H}, \\ \Pi_1 &= \frac{d}{H}, \\ \Pi_2 &= \frac{D}{H}, \\ \Pi_3 &= \theta, \\ \Pi_4 &= \rho_l^{\alpha_4} H^{\beta_4} \mu_l^{\gamma_4} P, \\ \Pi_5 &= \rho_l^{\alpha_5} H^{\beta_5} \mu_l^{\gamma_5} \mu_g, \\ \Pi_6 &= \rho_l^{\alpha_6} H^{\beta_6} \mu_l^{\gamma_6} \sigma_{g\text{-}l}, \\ \Pi_7 &= \rho_l^{\alpha_7} H^{\beta_7} \mu_l^{\gamma_7} \rho_g, \\ \Pi_8 &= \rho_l^{\alpha_8} H^{\beta_8} \mu_l^{\gamma_8} g, \\ \Pi_9 &= \rho_l^{\alpha_9} H^{\beta_9} \mu_l^{\gamma_9} v. \end{aligned} \tag{6}$$

For Π_4, plug in the dimensions of every variable; equation can be obtained as

$$\begin{aligned} &\left[M^0 L^0 T^0\right] \\ &= \left[ML^{-3}\right]^{\alpha_4} [L]^{\beta_4} \left[ML^{-1}T^{-1}\right]^{\gamma_4} \left[ML^{-1}T^{-2}\right]. \end{aligned} \tag{7}$$

The exponential equation set can be obtained as

$$\begin{aligned} M&: 0 = \alpha_4 + \gamma_4 + 1, \\ L&: 0 = -3\alpha_4 + \beta_4 - \gamma_4 - 1, \\ T&: 0 = -\gamma_4 - 2. \end{aligned} \tag{8}$$

Solve for $\alpha_4 = 1$, $\beta_4 = 2$, and $\gamma_4 = -2$. So $\Pi_4 = \rho_l H^2 \mu_l^{-2} P = \rho_l H^2 P / \mu_l^2$.

Similarly,

$$\begin{aligned} \Pi_5 &= \frac{\mu_g}{\mu_l}, \\ \Pi_6 &= \rho_l H \mu_l^{-2} \sigma_{g\text{-}l} = \frac{\rho_l H \sigma_{g\text{-}l}}{\mu_l^2}, \\ \Pi_7 &= \frac{\rho_g}{\rho_l}, \\ \Pi_8 &= \rho_l^2 H^3 \mu_l^{-2} g = \frac{\rho_l^2 H^3 g}{\mu_l^2}, \\ \Pi_9 &= \rho_l H \mu_l^{-1} v = \frac{\rho_l H v}{\mu_l}. \end{aligned} \tag{9}$$

So

$$f\left(\frac{d_B}{H}, \frac{d}{H}, \frac{D}{H}, \theta, \frac{\rho_l H^2 P}{\mu_l^2}, \frac{\mu_g}{\mu_l}, \frac{\rho_l H \sigma_{g\text{-}l}}{\mu_l^2}, \frac{\rho_g}{\rho_l}, \frac{\rho_l^2 H^3 g}{\mu_l^2}, \frac{\rho_l H v}{\mu_l}\right) = 0. \tag{10}$$

In order to get the expression of d_B, the average diameter of bubbles can be expressed as an explicit function:

$$\frac{d_B}{H} = f_1\left(\frac{d}{H}, \frac{D}{H}, \theta, \frac{\rho_l H^2 P}{\mu_l^2}, \frac{\mu_g}{\mu_l}, \frac{\rho_l H \sigma_{g\text{-}l}}{\mu_l^2}, \frac{\rho_g}{\rho_l}, \frac{\rho_l^2 H^3 g}{\mu_l^2}, \frac{\rho_l H v}{\mu_l}\right). \tag{11}$$

In addition, for the specific circumstances of our experimental study, where D, H, P, ρ_l, μ_l, ρ_g, μ_g, $\sigma_{g\text{-}l}$, and g are quantitative, (11) can be written as

$$\frac{d_B}{H} = f_2\left(\frac{d}{H}, \theta, \frac{\rho_l H v}{\mu_l}\right). \tag{12}$$

The above formula needs to be determined by experiments.

4. The Derivation of Empirical Formula

According to the established equations (11) and (12), combined with the specific conditions, the specific empirical formula can be derived [22–24].

In various phenomena, criterion equation can be expressed in the form of power function with the independent variable within a certain range. By the above analysis, empirical formula can be fitted:

$$\frac{d_B}{H} = A\left(\frac{d}{H}\right)^{b_1}(\theta)^{b_2}\left(\frac{\rho_l H\nu}{\mu_l}\right)^{b_3}. \quad (13)$$

Among them A, b_1, b_2, and b_3 are fitting coefficient.

Do logarithmic operations on the above formula; then

$$\ln\frac{d_B}{H} = \ln A + b_1\ln\frac{d}{H} + b_2\ln\theta + b_3\ln\frac{\rho_l H\nu}{\mu_l}. \quad (14)$$

Based on the linear relationship of the above form, fitting was carried out on the data of our injection experiment process [18].

The above fitting coefficients were obtained: $\ln A = 1.98584$, $A = 7.28519$, $b_1 = 0.29374$, $b_2 = -0.46572$, and $b_3 = -0.16725$. So

$$\ln\frac{d_B}{H} = 7.28519 + 0.29374\ln\frac{d}{H} - 0.46572\ln\theta - 0.16725\ln\frac{\rho_l H\nu}{\mu_l}. \quad (15)$$

So

$$\frac{d_B}{H} = 7.28519\left(\frac{d}{H}\right)^{0.29374}(\theta)^{-0.46572}\left(\frac{\rho_l H\nu}{\mu_l}\right)^{-0.16725}. \quad (16)$$

Then the empirical formula on average diameter of bubbles was established as

$$d_B = 7.28519H\left(\frac{d}{H}\right)^{0.29374}(\theta)^{-0.46572}\left(\frac{\rho_l H\nu}{\mu_l}\right)^{-0.16725}. \quad (17)$$

In this formula, H is a constant value which is equal to 0.36 m. ρ_l is the density of water which is equal to 1000 kg·m^{-3}. μ_l is the viscosity of water which is equal to 1.0×10^{-3} N·s·m^{-2}. So

$$d_B = 0.41666 d^{0.29374}\theta^{-0.46572}\nu^{-0.16725}. \quad (18)$$

It can be seen from the dimensionless criterion equation that, among the factors discussed, nozzle installing angle and diameter of nozzle make the most impact on the average diameter of bubbles in bottom blown oxygen copper furnace. There is a negative correlation between the nozzle installing angle and average diameter of bubbles. There is a positive correlation between the diameter of nozzle and the average diameter of bubbles.

Use the experimental results and the calculated results as the abscissa and ordinate, respectively, to plot a graph and compare with $y = x$. The results are shown in Figure 3. The experimental results accord with the calculated results well. So the model can predict the mean bubbles diameter in the water model of bottom blown furnace.

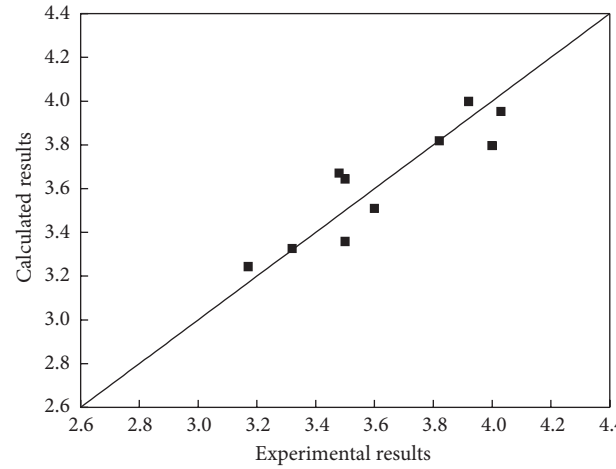

Figure 3: Relationship between experimental results and calculated results.

5. Discussions

5.1. Effects of Nozzle Diameter on the Average Diameters of Bubbles. The gas velocity was 340 m/s, and the angle between the nozzle and horizontal plane θ is 90°. With different diameters of the nozzles, the mean diameters of bubbles were measured in the experiment. From (18) and experimental conditions, (19) was obtained:

$$d_B = 0.019331 d^{0.29374}. \quad (19)$$

The predicted values by (19) and experimental results were shown in Figure 4. When the diameter of the nozzle increases, the mean diameter of bubbles has a trend of increase.

5.2. Effects of Angle between the Nozzle and Horizontal Plane on the Average Diameters of Bubbles. The gas velocity was 340 m/s, and the diameter of the nozzle was 3.0 mm. With different angles between the nozzles and horizontal plane, the mean diameters of bubbles were measured in the experiment. From (18) and experimental conditions, (20) was obtained:

$$d_B = 0.028531\theta^{-0.46572}. \quad (20)$$

The predicted values by (20) and experimental results were shown in Figure 5. As illustrated in Figure 5, with the increase of the angles, the mean diameter of bubbles has a decreasing tendency.

5.3. Effects of Gas Velocity on the Average Diameters of Bubbles. The angle between the nozzle and horizontal plane θ was 90° and the diameter of the nozzle was 3.0 mm. With different gas velocity, the mean diameters of bubbles were measured in the experiment. From (18) and experimental conditions, (21) was obtained:

$$d_B = 0.0093021\nu^{-0.16725}. \quad (21)$$

The predicted values by (20) and experimental results were shown in Figure 5. It can be seen from Figure 6 that

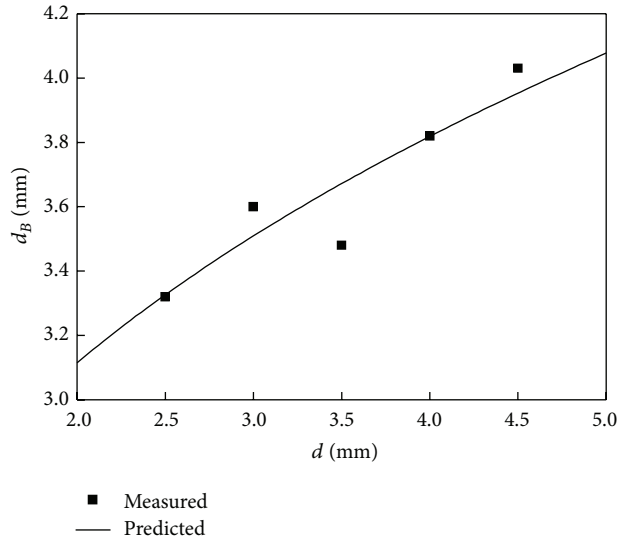

Figure 4: Effects of nozzle diameter on the average diameters of bubbles.

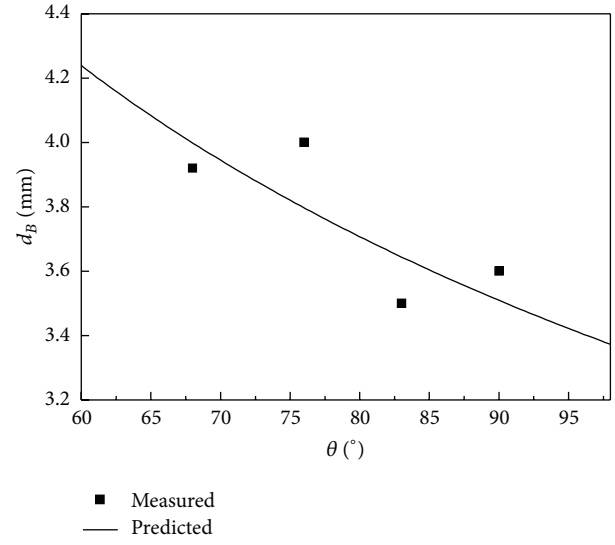

Figure 5: Effects of angle between the nozzle and horizontal plane on the mean diameters of bubbles.

the mean diameter of bubbles has a trend of decrease by the increasing of the gas velocity.

6. Bubbles in Industrial Conditions

The size and operating conditions of cold model are very different from those of actual industrial vessels. We will discuss the differences we expect between the cold model results and the industrial situation in the following part.

The flow characteristics of high temperature melt in metallurgical reactor are very difficult to be measured, especially for the measurement of internal bubble. Besides, the cost of high temperature experiment or industrial experiment is very high. Cold model experiment is an important method to research the flow phenomena in molten bath. Though there

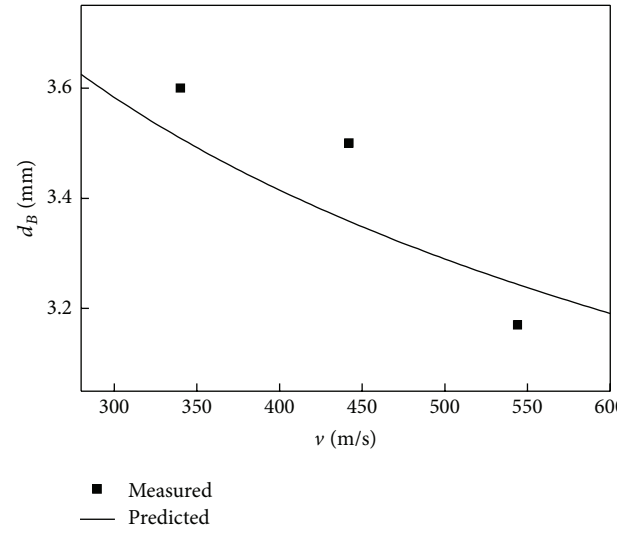

Figure 6: Effects of nozzle diameter on the mean diameters of bubbles.

is difference between cold model results and the industrial situation, cold model is an interim solution to research high temperature metallurgical reactor.

The cold water model we used follows the principle of similarity, including geometric similarity and dynamic similarity. Keeping the same Froude number allows the fluid flow patterns obtained in cold model similar with the industrial prototype [25].

For bottom gas injection, the bubble size in gas/water systems is different from that of gas/metal system, because the temperature, the density, and surface tension of liquid are different in the two systems.

Iguchi et al. [26] measured the bubble characteristics in a molten iron bath at the temperature of 1250°C in an experimental apparatus. To estimate the bubble size in bath due to a temperature difference, they measured the temperature of gas 75 mm upstream from the nozzle exit with a thermocouple and calculated that the temperature of gas 10 mm upstream from the nozzle exit is almost the same as the bath. In copper furnace, the temperature of bath is 1150~1200°C. But for the industrial situation, the gas flow rate is about 100 times higher than that in the water model, so the heat transfer conditions are different from the experiment. Only after the temperature of gas before or after the nozzle exit has been measured, some reliable estimations could be made. If the bubble formed after full heating, the gas flow rate or the velocity should be corrected according to the rise of gas temperature. If the bubble formed before full heating, its volume will expand according to the rise of temperature.

Liu et al. [27] discussed applicability of the water experimental results to the hot metal ladle in actual plant. They thought the differences in the surface tension and density of liquid should be taken into account in estimating the bubble size in molten iron on the basis of the present water model experiment. For molten iron, ρ/σ (surface tension/density) is 3.5 times that of water and they obtained the relation that the diameter of bubble in plant is 0.34 times that of the bubble in

water model according to predecessors' empirical equation. But they did not take the temperature into account. In this paper, for the copper smelting system, ρ/σ nearly equals (is about 0.95 times) that of the water system, so the effect of surface tension/density is little. But the surface tension and density are affected greatly by the grade and elements of copper matte. This increases the difficulty of estimating the diameter of bubble in the actual plant.

Besides cold model experiment, CFD (Computational Fluid Dynamics) is an important method to investigate flow phenomena in reactors. To investigate the bubble size in high temperature industrial situation, firstly, a water model should be built. The characteristics of bubbles will be studied in cold model experiments, as shown in this paper. Secondly, a numerical model of water model will be established. The experimental results of cold model will be used to verify the numerical model. The validated numerical model will be used to study the characteristics of bubbles in the industrial situation, and the temperature, the surface tension, and density of liquid can be taken into account. Li et al. [28] used water model experiment to validate the mathematical model and then a CFD-PBM coupled model was used to calculate the gas bubble size distribution. Liu et al. [29] developed a three-dimensional mathematical model for simulation of flow, temperature, and concentration fields in a pilot-scale rotary hearth furnace using a commercial CFD software, FLUENT.

The relationship of bubble size between gas/water and gas/metal systems is an issue which has puzzled researchers for decades. Many people made a lot of meaningful attempts, but for the complex forming process of bubbles and insufficient consideration of the factors affecting the bubbles, no accurate predicting methods have been proposed till now.

As a conclusion, before the measurement of bubble characteristics, or at least the temperature fields, the surface tension, and density of copper matte in a particular industrial situation, it is very difficult for us to quantitatively predict the bubble size in industrial situation through the result of water model experiment. But as the cold model experiment met the principle of similarity. The results obtained from the present cold model can be used to predict the changing tendency of bubble size in the industrial situation, at least qualitatively. And the results can be used to verify the numerical model which will be applied to investigate the industrial situation.

7. Conclusions

By the method of dimensional analysis and Buckingham's theorem, the influence of different experimental conditions on the average diameter of bubbles can be studied and the fitting equation was obtained. Do fitting on the data of our experiment, fitting coefficients were obtained, and then the empirical formula on average diameter of bubbles was established as

$$d_B = 0.41666 d^{0.29374} \theta^{-0.46572} \nu^{-0.16725}. \quad (22)$$

In this formula, the power exponent of θ is equal to -0.46572, which has the maximum absolute value. So there is a negative correlation between the nozzle installing angle and average diameter of bubbles. Then the diameter of nozzle makes the second most impact on the average diameter of bubbles and there is a positive correlation between them. This model can be used to predict the mean bubbles diameter in the water model of bottom blown furnace.

Competing Interests

The authors declare that they have no competing interests.

Acknowledgments

This research was financially supported by the Joint Funds of the National Natural Science Foundation of China (U1402271, U1202274, and 51204040), National 863 Plan (2012AA062303), the National Science and Technology Support Program (2012BAE01B02), and Fundamental Research Funds for the Central Universities (N100302005).

References

[1] W. G. Davenport, M. King, M. Schlesinger, and A. K. Biswas, *Extractive Metallurgy of Copper*, Pergamon Press, Elsevier Science, Kidlington, UK, 4th edition, 2002.

[2] International Copper Study Group, *The World Copper Factbook 2014*, 2014.

[3] C. A. Llanos, S. Garcia-Hernandez, J. A. Ramos-Banderas, J. J. de Barreto, and G. Solorio-Diaz, "Multiphase modeling of the fluidynamics of bottom argon bubbling during ladle operations," *ISIJ International*, vol. 50, no. 3, pp. 396–402, 2010.

[4] B. Li, H. Yin, C. Q. Zhou, and F. Tsukihashi, "Modeling of three-phase flows and behavior of slag/steel interface in an argon gas stirred ladle," *ISIJ International*, vol. 48, no. 12, pp. 1704–1711, 2008.

[5] A.-H. Jiang, S.-H. Yang, C. Mei, Z.-M. Shi, and X.-J. Zhu, "Exergy analysis of oxygen bottom blown furnace in SKS lead smelting system," *Journal of Central South University (Science and Technology)*, vol. 41, no. 3, pp. 1190–1195, 2010.

[6] L. Hu and D. Li, "Development and application of oxygen bottom blowing melting furnace," *Non-Ferrous Metallurgical Equipment*, no. 1, pp. 34–53, 2011.

[7] Y. Liang, Z. Cai, Z. Qian et al., "Model study on the continuous oxygen bottom blowing lead-making process II. The optimum dam location," *Chemical Metallurgy*, vol. 7, no. 1, pp. 45–53, 1986.

[8] B. Zhao, Z. Cui, and Z. Wang, "A new copper smelting technology-bottom blown oxygen furnace developed at dongying fangyuan nonferrous metals," in *Proceedings of the TMS Annual Meeting 2013, 4th International Symposium on High-Temperature Metallurgical Processing*, pp. 3–10, 2013.

[9] J. Jiang, "The new technology and device of continuous copper smelting using oxygen bottom blown furnace," *China Metal Bulletin*, vol. 17, pp. 29–31, 2008.

[10] Shandong Fangyuan Nonferrous Metals Group and China ENFI Engineering Corporation, "The industrial practice of oxygen bottom blown smelting technology for polymetallic resources," *Resource Recycling*, no. 11, pp. 46–49, 2009.

[11] J. K. Walters and J. F. Davidson, "The initial motion of a gas bubble formed in an inviscid liquid Part 1. The two-dimensional

bubble," *Journal of Fluid Mechanics*, vol. 12, no. 3, pp. 408–416, 1962.

[12] J. K. Walters and J. F. Davidson, "The initial motion of a gas bubble formed in an inviscid liquid Part 2. The three-dimensional bubble and the toroidal bubble," *Journal of Fluid Mechanics*, vol. 17, no. 3, pp. 321–336, 1963.

[13] E. O. Hoefele and J. K. Brimacombe, "Flow regimes in submerged gas injection," *Metallurgical Transactions B*, vol. 10, no. 4, pp. 631–648, 1979.

[14] A. A. Bustos, G. G. Richards, N. B. Gray, and J. K. Brimacombe, "Injection phenomena in nonferrous processes," *Metallurgical Transactions B*, vol. 15, no. 1, pp. 77–89, 1984.

[15] A. Valencia, M. Rosales-Vera, and C. Orellana, "Fluid dynamics in a teniente type copper converter model with one and two tuyeres," *Advances in Mechanical Engineering*, no. 1, pp. 323–335, 2013.

[16] Y.-F. Zhao and G. A. Irons, "The breakup of bubbles into jets during submerged gas injection," *Metallurgical Transactions B*, vol. 21, no. 6, pp. 997–1003, 1990.

[17] W.-T. Lou, B.-Q. Zhang, and Z. Shi, "Simulation of bubble dynamics in water model of ISA vessel," *China Nonferrous Metallurgy*, no. 1, pp. 48–53, 2010.

[18] D. Wang, Y. Liu, Z. Zhang, P. Shao, and T. Zhang, "Experimental study of bottom blown oxygen copper smelting process for water model," in *Proceedings of the 7th International Conference on Micromechanics of Granular Media (Powders and Grains)*, vol. 1542, pp. 1304–1307, Sydney, Australia, July 2013.

[19] L.-L. Wang, X.-D. Yong, R. Li, and Q. Ma, "Image processing technology in the application of bubble characteristics research," *Journal of Sichuan University (Engineering Science Edition)*, vol. 44, no. 2, pp. 188–192, 2012.

[20] E.-R. Avram, E. Mamut, L. Oancea, and C. Bâcu, "The method of dimensional analysis using similitude theory applied for modeling of fluid flow in microchannels," in *Proceedings of the 7th International Symposium on Advanced Topics in Electrical Engineering (ATEE '11)*, pp. 1–6, Bucharest, Romania, May 2011.

[21] G. Mary, S. Mezdour, G. Delaplace, R. Lauhon, G. Cuvelier, and F. Ducept, "Modelling of the continuous foaming operation by dimensional analysis," *Chemical Engineering Research and Design*, vol. 91, no. 12, pp. 2579–2586, 2013.

[22] Y. Liu, Y. Li, T. Zhang, and N. Feng, "Research on the penetration depth in aluminum reduction cell with new type of anode and cathode structures," *JOM*, vol. 66, no. 7, pp. 1202–1209, 2014.

[23] Z. Zhang, *The Principle of Dimensional Analysis*, People's Railway Press, Beijing, China, 1979.

[24] Y. Liu, T. Zhang, Q. Wang, W. Yao, M. Sano, and J. He, "Dimension analysis theory in the application of fluid mechanics," *Industrial Furnace*, vol. 29, no. 6, pp. 9–12, 2007 (Chinese).

[25] G. Solorio-Díaz, R. D. Morales, and A. Ramos-Banderas, "Effect of a swirling ladle shroud on fluid flow and mass transfer in a water model of a tundish," *International Journal of Heat and Mass Transfer*, vol. 48, no. 17, pp. 3574–3590, 2005.

[26] M. Iguchi, H. Kawabata, Y. Ito, K. Nakajima, and Z.-I. Morita, "Continuous measurements of bubble characteristics in a molten iron bath with Ar gas injection," *ISIJ International*, vol. 34, no. 12, pp. 980–985, 1994.

[27] Y. Liu, M. Sano, T. A. Zhang, Q. Wang, and J. He, "Intensification of bubble disintegration and dispersion by mechanical stirring in gas injection refining," *ISIJ International*, vol. 49, no. 1, pp. 17–23, 2009.

[28] L. Li, Z. Liu, B. Li, H. Matsuura, and F. Tsukihashi, "Water model and CFD-PBM coupled model of gas-liquid-slag three-phase flow in ladle metallurgy," *ISIJ International*, vol. 55, no. 7, pp. 1337–1346, 2015.

[29] Y. Liu, F.-Y. Su, Z. Wen, Z. Li, H.-Q. Yong, and X.-H. Feng, "CFD modeling of flow, temperature, and concentration fields in a pilot-scale rotary hearth furnace," *Metallurgical and Materials Transactions B*, vol. 45, no. 1, pp. 251–261, 2014.